European Journal of Mechanics B/Fluids 28 (2009) 605–612

Contents lists available at ScienceDirect

European Journal of Mechanics B/Fluids

journal homepage: www.elsevier.com/locate/ejmflu

Stability of bichromatic gravity waves on deep water

Stéphane Leblanc

LSEET/CNRS, University of Toulon, F-83957 La Garde cedex, France

ARTICLE INFO

Article history:
Received 19 December 2008
Received in revised form
14 April 2009
Accepted 6 May 2009
Available online 18 May 2009

Keywords:
Gravity waves
Modulational instability
Nonlinear interactions

ABSTRACT

The stability of bichromatic gravity waves with small but finite amplitudes propagating in two directions on deep water is considered. Starting from the Zakharov equation, elementary quartet interactions are isolated and stability criteria are formulated. Results are illustrated for various combinations of bichromatic wave trains, from long-crested to standing waves. Two generic mechanisms operate: the first one is a modulational instability of one of the two components of the bichromatic wave train; the second mechanism is a modulation which couples both components of the wave train. However a third mechanism eventually comes into play: the resonant interaction of Phillips and Longuet-Higgins which leads initially to the linear growth of a third wave. When this latter is active, in particular for wave trains with wave vectors close together, it is shown by numerical integration that the long-time recurrence is destroyed.

1. Introduction

In deep water, finite amplitude gravity waves—*i.e.* Stokes waves—are known to be unstable to disturbances that modulate the initial wave train. This is the instability described by Benjamin and Feir [1] with a classical stability analysis, and by Benney and Newell [2] using a nonlinear Schrödinger equation. In the same time, Phillips [3] and Zakharov [4] understood that this modulational instability could be described in terms of nonlinear interactions between the Stokes wave with wave vector $\boldsymbol{k}_0$, and two sideband disturbances with wave vectors $\boldsymbol{k}_1$ and $\boldsymbol{k}_2$, providing that the wave vectors and the frequencies satisfy approximately the resonance condition:

$$\boldsymbol{k}_1 + \boldsymbol{k}_2 = 2\boldsymbol{k}_0, \quad \omega(\boldsymbol{k}_1) + \omega(\boldsymbol{k}_2) = 2\omega(\boldsymbol{k}_0).$$

Using Zakharov's formulation, the instability increments computed by Crawford et al. [5] and compared to the numerical results of Longuet-Higgins [6] have demonstrated the accuracy of weakly nonlinear theory to describe modulational instability. Surveys and recent developments may be found in Refs [7–13]. Note that a rigorous proof of the Benjamin–Feir instability has been established by Bridges and Mielke [14].

For wave trains propagating in two directions with different amplitudes and wavelengths, giving rise to two dimensional surface patterns on a three-dimensional flow, stability theory is generally restricted to long wavelength modulations described essentially by coupled nonlinear Schrödinger (NLS) equations [15–19]. Okamura [20] used however the Zakharov equation to study the stability of standing waves and observed two types of modes characterized by different quartet interactions. Similar modes were observed numerically by Ioualalen and Kharif [21,22] for waves with same wavelength and amplitude propagating in different directions (long- and short-crested waves), and by Badulin et al. [23] using Zakharov's formulation. These two types of instability may be described as follows: the first one ('class Ia') corresponds to full resonant interaction between the two primary waves and the disturbances, and the second one ('class Ib') is a modulational instability associated to each component separately. For steeper bichromatic wave trains, 'class II' instabilities are described in Ref. [24].

Mathematical aspects of the stability of standing and short-crested waves using Hamiltonian theory are presented by Bridges and Laine-Pearson [25,26]. It is shown in particular that the coupled NLS equations derived by Okamura [20] for standing waves have to be replaced by nonlocal amplitude equations derived by Pierce and Knobloch [17]. For short-crested waves, it is also shown that the coupled NLS equations of Roskes [15] miss out some instabilities. I shall not pursue this interesting discussion since the method used here has a higher accuracy than those based on NLS equations.

Indeed, in the present study, the approach of Crawford et al. [5], Okamura [20], and Badulin et al. [23] based on Zakharov's formulation is applied to bichromatic waves with arbitrary amplitudes, wavelengths, and directions. Explicit formulas for growth rates are derived, and long-time numerical integrations are performed. Finally, the resonant interaction discovered by Phillips and

E-mail address: sl@univ-tln.fr

0997-7546/$ – see front matter © 2009 Elsevier Masson SAS. All rights reserved.
doi:10.1016/j.euromechflu.2009.05.001

Longuet-Higgins [27–31], which in a bichromatic wave train leads to the growth of a third wave, is discussed. It is shown that its interaction with the modulational instability destroys the usual recurrence cycle.

2. The bichromatic wave train

Deep-water irrotational gravity waves propagating at the surface of an inviscid incompressible fluid are governed, at third order in amplitude, by an equation first derived by Zakharov [4]:

$$i\partial_t b(\boldsymbol{k},t) = \omega(\boldsymbol{k})b(\boldsymbol{k},t) + \int_{\boldsymbol{k}+\boldsymbol{p}=\boldsymbol{q}+\boldsymbol{r}} T(\boldsymbol{k},\boldsymbol{p},\boldsymbol{q},\boldsymbol{r})b^*(\boldsymbol{p},t)b(\boldsymbol{q},t)b(\boldsymbol{r},t)\,d\boldsymbol{p}\,d\boldsymbol{q}\,d\boldsymbol{r}, \quad (1)$$

where $\omega(\boldsymbol{k}) = (g|\boldsymbol{k}|)^{1/2}$, and $T(\boldsymbol{k},\boldsymbol{p},\boldsymbol{q},\boldsymbol{r})$ is Krasitskii's kernel [32] given in Appendix. The spectral variable $b(\boldsymbol{k},t)$ is related, at leading order, to the free-surface elevation $\eta(\boldsymbol{x},t)$ by:

$$\eta(\boldsymbol{x},\boldsymbol{t}) = \int \left(\frac{|\boldsymbol{k}|}{2\omega(\boldsymbol{k})}\right)^{\frac{1}{2}} \left(b(\boldsymbol{k},t) + b^*(-\boldsymbol{k},t)\right) e^{i\boldsymbol{k}\cdot\boldsymbol{x}} d\boldsymbol{k}.$$

According to Zakharov [4], the simplest solution of (1) is

$$b(\boldsymbol{k},t) = b_0(t)\delta(\boldsymbol{k}-\boldsymbol{k}_0), \quad b_0(t) = B_0 e^{-i\Omega_0 t},$$
$$\Omega_0 = \omega_0 + T_{00}|B_0|^2, \quad (2)$$

where $\omega_i = \omega(\boldsymbol{k}_i)$ and $T_{ii} = T(\boldsymbol{k}_i,\boldsymbol{k}_i,\boldsymbol{k}_i,\boldsymbol{k}_i) = k_i^3$, with $k_i = |\boldsymbol{k}_i|$. In terms of free surface elevation, this corresponds at leading order to:

$$\eta(\boldsymbol{x},t) = a_0 \cos(\boldsymbol{k}_0\cdot\boldsymbol{x} - \Omega_0 t + \varphi_0), \quad \Omega_0 = \omega_0\left(1 + \frac{1}{2}k_0^2 a_0^2\right),$$

where here and below $a_i = (2k_i/\omega_i)^{1/2}|B_i|$ and $\varphi_i = \arg(B_i)$. This is Stokes wave.

Another simple solution is the combination of two waves $\mathbf{k}_1 \neq \mathbf{k}_2$ [33]:

$$\left.\begin{aligned} b(\boldsymbol{k},t) &= b_1(t)\delta(\mathbf{k}-\mathbf{k}_1) + b_2(t)\delta(\mathbf{k}-\mathbf{k}_2),\\ b_1(t) &= B_1 e^{-i\Omega_1 t}, \quad \Omega_1 = \omega_1 + T_{11}|B_1|^2 + 2T_{12}|B_2|^2,\\ b_2(t) &= B_2 e^{-i\Omega_2 t}, \quad \Omega_2 = \omega_2 + T_{22}|B_2|^2 + 2T_{21}|B_1|^2, \end{aligned}\right\} \quad (3)$$

where $T_{ij} = T(\boldsymbol{k}_i,\boldsymbol{k}_j,\boldsymbol{k}_i,\boldsymbol{k}_j) = T_{ji}$ is given in symmetric form by:

$$T_{ij} = -\frac{1}{4(k_ik_j)^{\frac{1}{2}}}\Big\{3(k_ik_j)^2 + (\boldsymbol{k}_i\cdot\boldsymbol{k}_j)\Big(\boldsymbol{k}_i\cdot\boldsymbol{k}_j - 4(k_i+k_j)(k_ik_j)^{\frac{1}{2}}\Big) + \frac{2(\omega_i-\omega_j)^2(\boldsymbol{k}_i\cdot\boldsymbol{k}_j + k_ik_j)^2}{g|\boldsymbol{k}_i-\boldsymbol{k}_j| - (\omega_i-\omega_j)^2} + \frac{2(\omega_i+\omega_j)^2(\boldsymbol{k}_i\cdot\boldsymbol{k}_j - k_ik_j)^2}{g|\boldsymbol{k}_i+\boldsymbol{k}_j| - (\omega_i+\omega_j)^2}\Big\} \quad (4)$$

In physical space, (3) corresponds at leading order to:

$$\eta(\boldsymbol{x},t) = a_1\cos(\boldsymbol{k}_1\cdot\boldsymbol{x} - \Omega_1 t + \varphi_1) + a_2\cos(\boldsymbol{k}_2\cdot\boldsymbol{x} - \Omega_2 t + \varphi_2).$$

This is the bichromatic wave train first considered by Longuet-Higgins and Phillips [29]. Note that $T_{12} = -k_1^3 = -k_2^3$ when $\boldsymbol{k}_2 = -\boldsymbol{k}_1$ and (3) represents a standing wave. Recall also that (3) is not valid when $\boldsymbol{k}_2 = \boldsymbol{k}_1$, but the flow in that case is a Stokes wave with amplitude $a_0 = a_1 + a_2$. Matching between long-crested and Stokes waves is discussed by Roberts and Peregrine [34].

3. Modulational instability of a single wave train

When three waves $(\boldsymbol{k}_0,\boldsymbol{k}_1,\boldsymbol{k}_2)$ interact resonantly, their amplitude is no longer steady contrary to two waves. This happens for instance when $2\boldsymbol{k}_0 = \boldsymbol{k}_1 + \boldsymbol{k}_2$. The Zakharov equation (1) then reduces to the discrete system [3,35]:

$$\left.\begin{aligned} i\dot{b}_0 &= \Gamma_0 b_0 + 2T_{0012}b_0^* b_1 b_2,\\ i\dot{b}_1 &= \Gamma_1 b_1 + T_{0012}b_2^* b_0^2,\\ i\dot{b}_2 &= \Gamma_2 b_2 + T_{0012}b_1^* b_0^2, \end{aligned}\right\} \quad (5)$$

where $\Gamma_i = \omega_i + T_{ii}|b_i|^2 + 2\sum_{j\neq i} T_{ij}|b_j|^2$ and $T_{ijmn} = T(\boldsymbol{k}_i,\boldsymbol{k}_j,\boldsymbol{k}_m,\boldsymbol{k}_n)$.

If $\sup\{|b_1|,|b_2|\} \ll |b_0|$ initially, then the system may be linearized for short time and the first equation of (5) admits Stokes wave (2) as solution. After setting

$$b_1(t) = B_1 e^{\sigma t} e^{-\frac{i}{2}\Delta_{0012}t} e^{-i\Omega_1 t}, \quad \Omega_1 = \omega_1 + 2T_{10}|B_0|^2,$$
$$b_2(t) = B_2 e^{\sigma^* t} e^{-\frac{i}{2}\Delta_{0012}t} e^{-i\Omega_2 t}, \quad \Omega_2 = \omega_2 + 2T_{20}|B_0|^2,$$

where $\Delta_{ijmn} = \Omega_i + \Omega_j - \Omega_m - \Omega_n$, exponential growth at rate σ occurs when

$$\sigma^2 = T_{0012}^2|B_0|^4 - \frac{1}{4}\Delta_{0012}^2 > 0. \quad (6)$$

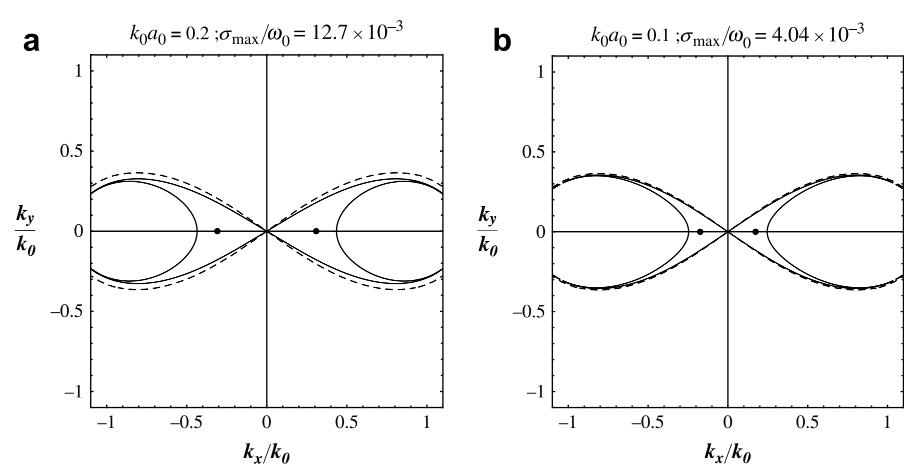

Fig. 1. Modulational instability of Stokes wave $\boldsymbol{k}_0 = (k_0, 0)$ for different steepnesses k_0a_0. Solid lines represent the stability boundaries from (7), dashed lines Phillips resonant curves (7), and the dots the maximum growth rates. The wave vector $\boldsymbol{k} = (k_x, k_y)$ is defined by $\boldsymbol{k} = \boldsymbol{k}_1 - \boldsymbol{k}_0$.

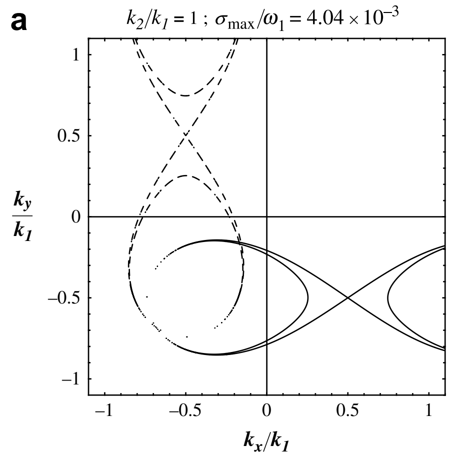

Fig. 2. Class Ib instabilities of bichromatic waves $\boldsymbol{k}_1 = (k_1, 0)$ and $\boldsymbol{k}_2 = (k_2 \cos\theta, k_2 \sin\theta)$ with steepnesses $k_1a_1 = k_2a_2 = 0.1$ and $\theta = 90°$. Solid (resp. dashed) lines represent the stability boundaries from (10) (resp. (13)) for the modulations of wave k_1 (resp. k_2); the wave vector $\boldsymbol{k} = (k_x, k_y)$ is defined by $\boldsymbol{k} = \boldsymbol{k}_3 - \frac{1}{2}(\boldsymbol{k}_1 + \boldsymbol{k}_2)$.

Since $\Delta_{0012} = 2\omega_0 - \omega_1 - \omega_2 + O(k_0^3|B_0|^2)$, this resonance occurs in the vicinity of the curves defined in k-space by:

$$2\boldsymbol{k}_0 = \boldsymbol{k}_1 + \boldsymbol{k}_2, \quad 2\omega_0 = \omega_1 + \omega_2, \tag{7}$$

which are Phillips 'figures-of-eight' [27]. Computations were first performed by Crawford et al. [5]. Typical results are plotted in Fig. 1.

4. Class Ib instabilities in bichromatic wave trains

We consider now the evolution of quartets of waves ($\boldsymbol{k}_1$,$\boldsymbol{k}_2$,$\boldsymbol{k}_3$,$\boldsymbol{k}_4$) in which various interactions are possible. Assuming at first that the wave vectors satisfy $2\boldsymbol{k}_1 = \boldsymbol{k}_3 + \boldsymbol{k}_4$, the Zakharov equation then gives:

$$\left.\begin{aligned} i\dot{b}_1 &= \Gamma_1 b_1 + 2T_{1134} b_1^* b_3 b_4, \\ i\dot{b}_2 &= \Gamma_2 b_2, \\ i\dot{b}_3 &= \Gamma_3 b_3 + T_{1134} b_4^* b_1^2, \\ i\dot{b}_4 &= \Gamma_4 b_4 + T_{1134} b_3^* b_1^2. \end{aligned}\right\} \tag{8}$$

If $\sup\{|b_3|, |b_4|\} \ll \inf\{|b_1|, |b_2|\}$ at the initial time then, after linearization, the first two are satisfied by the bichromatic wave (3). After substituting

$$\left.\begin{aligned} b_3(t) &= B_3 e^{\sigma t} e^{-\frac{i}{2}\Delta_{1134} t} e^{-i\Omega_3 t}, \quad \Omega_3 = \omega_3 + 2T_{31}|B_1|^2 + 2T_{32}|B_2|^2, \\ b_4(t) &= B_4 e^{\sigma^* t} e^{-\frac{i}{2}\Delta_{1134} t} e^{-i\Omega_4 t}, \quad \Omega_4 = \omega_4 + 2T_{41}|B_1|^2 + 2T_{42}|B_2|^2, \end{aligned}\right\} \tag{9}$$

in the two remaining equations, it is found the disturbance ($\boldsymbol{k}_3$,$\boldsymbol{k}_4$) grows exponentially when

$$\sigma^2 = T_{1134}^2 |B_1|^4 - \frac{1}{4}\Delta_{1134}^2 > 0. \tag{10}$$

This occurs in the vicinity of the resonant curves

$$2\boldsymbol{k}_1 = \boldsymbol{k}_3 + \boldsymbol{k}_4, \quad 2\omega_1 = \omega_3 + \omega_4. \tag{11}$$

Thus the component $\boldsymbol{k}_1$ of the bichromatic wave train is unstable to sidebands ($\boldsymbol{k}_3$,$\boldsymbol{k}_4$), exactly as for the modulational instability. The growth rate differs slightly however.

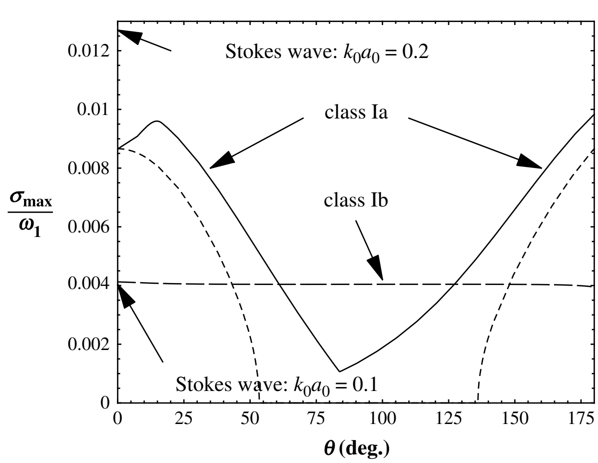

Fig. 3. Maximum growth rates of class Ia and Ib instabilities in bichromatic waves with steepnesses $k_1a_1 = k_2a_2 = 0.1$ and $k_1 = k_2$. Dashed lines correspond to long modulations (18).

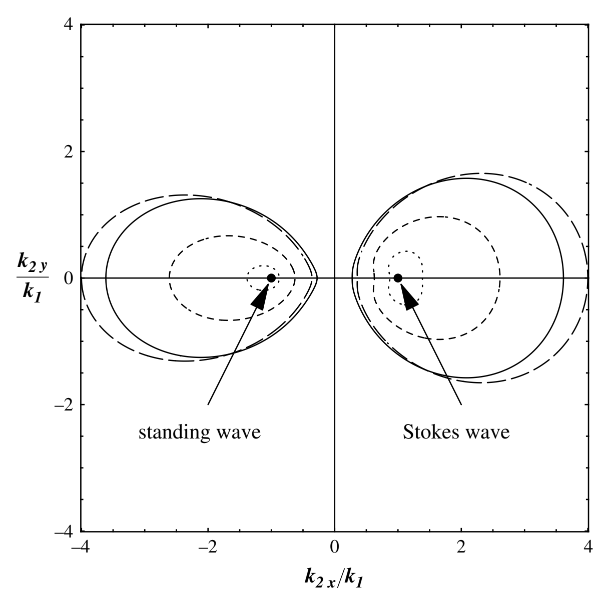

Fig. 4. Class Ia instabilities with long modulations according to (18) for bichromatic waves $\boldsymbol{k}_1 = (k_1, 0)$ and $\boldsymbol{k}_2 = (k_{2x}, k_{2y})$ with various steepness ratios $(k_2a_2)/(k_1a_1) = 1$ (solid lines), 0.7 (long-dashed lines), 0.4 (dashed lines), and 0.3 (dotted lines). The dots correspond to Stokes wave ($\boldsymbol{k}_2 = \boldsymbol{k}_1$) and standing wave ($\boldsymbol{k}_2 = -\boldsymbol{k}_1$).

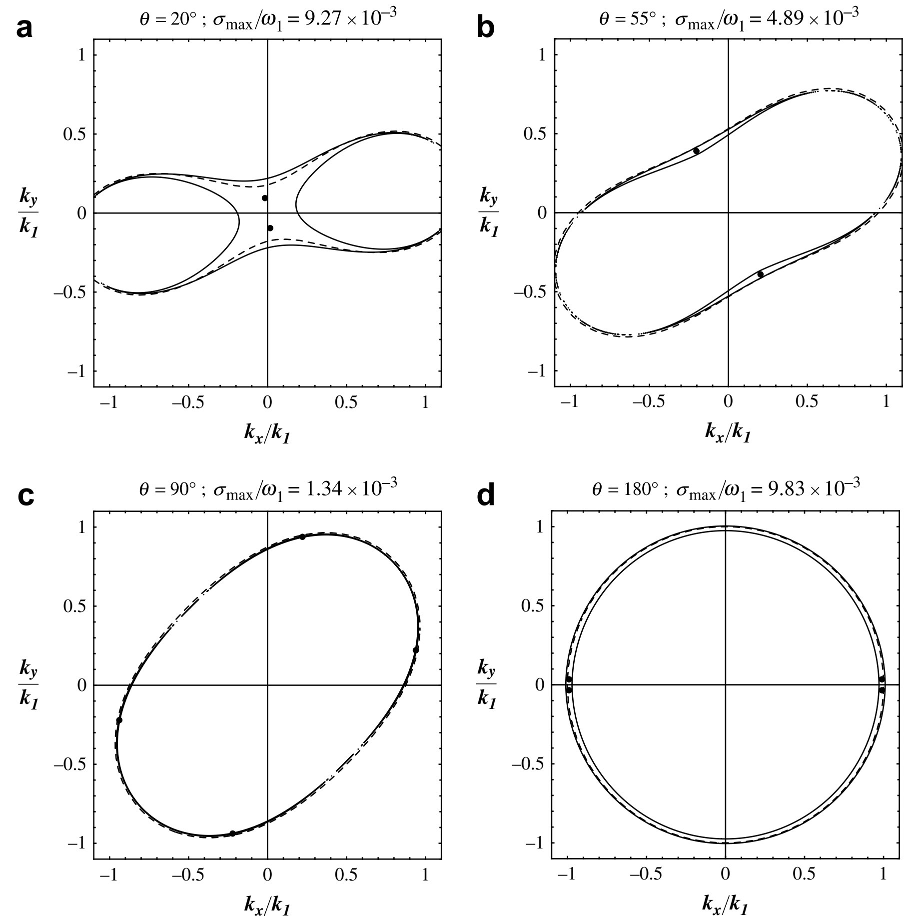

Fig. 5. Class Ia instabilities of bichromatic waves $\boldsymbol{k}_1 = (k_1, 0)$ and $\boldsymbol{k}_2 = (k_2 \cos\theta, k_2 \sin\theta)$ with steepnesses $k_1 a_1 = k_2 a_2 = 0.1$ and $k_1 = k_2$. Solid lines represent the stability boundaries from (16), dashed lines the resonant curves (16), and the dots the maximum growth rates. The wave vector $\boldsymbol{k} = (k_x, k_y)$ is defined by $\boldsymbol{k} = \boldsymbol{k}_3 - \frac{1}{2}(\boldsymbol{k}_1 + \boldsymbol{k}_2)$.

The same mechanism holds for the component $\boldsymbol{k}_2$ around the resonance

$$2\boldsymbol{k}_2 = \boldsymbol{k}_3 + \boldsymbol{k}_4, \quad 2\omega_2 = \omega_3 + \omega_4, \tag{12}$$

when

$$\sigma^2 = T_{2234}^2 |B_2|^4 - \frac{1}{4}\Delta_{2234}^2 > 0. \tag{13}$$

Both modes associated to components $\boldsymbol{k}_1$ and $\boldsymbol{k}_2$ correspond to 'type A' in the classification of Okamura [20] for standing waves, and to 'class Ib' in Ioualalen and Kharif [22] for long- and short-crested waves. To avoid confusions, the latter terminology is used here.

Typical results are presented in Fig. 2: it is seen that two similar patterns develop, one for each component of the bichromatic wave, having the same orientations than the components of the two primary waves. When they have the same steepness and wave-number, both class Ib instabilities have the same growth rate

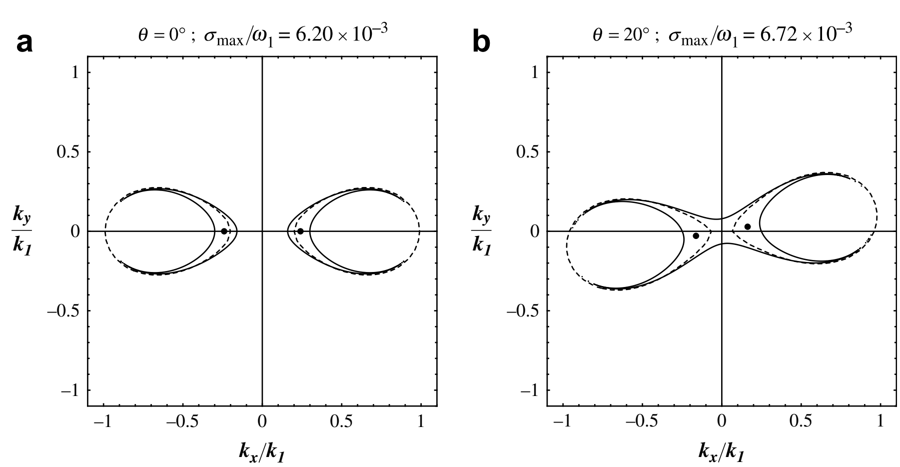

Fig. 6. Same as Fig. 5 for $k_2/k_1 = 0.6$.

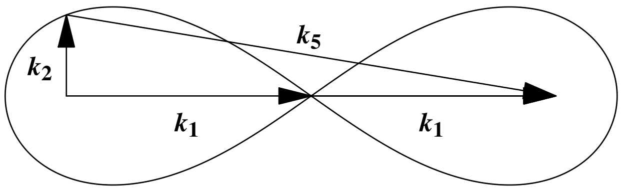

Fig. 7. Phillips figure-of-eight for the resonant interaction (20).

(Fig. 2a) and the patterns are almost identical than Fig. 1b corresponding to a single Stokes wave with same characteristics. Furthermore, the growth rate remains almost constant as the orientation of the crossing waves varies (Fig. 3). These observations are in agreement with the results of Badulin et al. [23]. Finally, Fig. 2b shows that the pattern associated to wave $\boldsymbol{k}_1$ is not affected when the wavelength of component $\boldsymbol{k}_2$ varies, and this holds for any orientation.

As a consequence, class Ib instability is a robust mechanism which affects each component of ($\boldsymbol{k}_1$,$\boldsymbol{k}_2$) independently. For long modulations, near the resonance (11) for instance, we set $\boldsymbol{k}_3 = \boldsymbol{k}_1 + \xi$ and $\boldsymbol{k}_4 = \boldsymbol{k}_1 - \xi$ and expand (10) in powers of $|B_1|$ and ξ. We get:

$$\sigma^2 = k_1^3|B_1|^2\delta_1^2 - \frac{1}{4}\delta_1^4, \quad \delta_1^2 = \frac{1}{4}\left(\omega_1/k_1^2\right)\left(\xi_{\parallel}^2 - 2\xi_{\perp}^2\right),$$

where $\xi_{\parallel}$ (resp. $\xi_{\perp}$) is the projection of ξ parallel (resp. perpendicular) to $\boldsymbol{k}_1$. Therefore, wave $\boldsymbol{k}_1$ is unstable to long modulations providing that its amplitude is sufficiently weak, and similarly for k_2, in agreement with Craig et al. [19].

5. Class Ia instabilities in bichromatic wave trains

Turning now to a quartet ($\boldsymbol{k}_1$,$\boldsymbol{k}_2$,$\boldsymbol{k}_3$,$\boldsymbol{k}_4$) in which the full interaction $\boldsymbol{k}_1 + \boldsymbol{k}_2 = \boldsymbol{k}_3 + \boldsymbol{k}_4$ occurs, the Zakharov equation gives [39,40]:

$$\left.\begin{aligned} i\dot{b}_1 &= \Gamma_1 b_1 + 2T_{1234}b_2^* b_3 b_4, \\ i\dot{b}_2 &= \Gamma_2 b_2 + 2T_{1234}b_1^* b_3 b_4, \\ i\dot{b}_3 &= \Gamma_3 b_3 + 2T_{1234}b_4^* b_1 b_2, \\ i\dot{b}_4 &= \Gamma_4 b_4 + 2T_{1234}b_3^* b_1 b_2. \end{aligned}\right\} \tag{14}$$

After linearization around (3), the disturbance (9) grows exponentially when

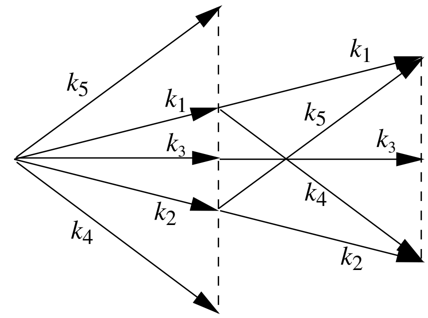

Fig. 9. Coupled quartet interactions (21) in a five-wave system.

$$\sigma^2 = 4T_{1234}^2|B_1|^2|B_2|^2 - \frac{1}{4}\Delta_{1234}^2 > 0. \tag{15}$$

From the definitions of Δ_{1234} and Ω_i in (3) and (9), it is clear that the unstable regions in wave vector plane lie in the vicinity of the resonant curves

$$\boldsymbol{k}_1 + \boldsymbol{k}_2 = \boldsymbol{k}_3 + \boldsymbol{k}_4, \quad \omega_1 + \omega_2 = \omega_3 + \omega_4, \tag{16}$$

first described and represented by Hasselmann [36–38]. This instability belongs to 'class Ia' in the classification Ioualalen and Kharif ('type B' of Okamura).

A simple criterion may be derived for long modulations. If we set $\boldsymbol{k}_3 = \boldsymbol{k}_1 + \xi$ and $\boldsymbol{k}_4 = \boldsymbol{k}_2 - \xi$ with $\xi \ll \inf\{k_1, k_2\}$, and expand (15) up to the fourth order in amplitude and to the second order in ξ, we get:

$$\sigma^2 = 4T_{12}^2|B_1|^2|B_2|^2 - \frac{1}{4}\left\{\left(\frac{\omega_2\boldsymbol{k}_2}{2k_2^2} - \frac{\omega_1\boldsymbol{k}_1}{2k_1^2}\right)\cdot\xi - k_1^3|B_1|^2 - k_2^3|B_2|^2\right\}^2. \tag{17}$$

For fixed amplitudes $|B_1|$ and $|B_2|$, and wave vectors $\boldsymbol{k}_1$ and $\boldsymbol{k}_2$, the maximum growth rate is then reach when the scalar product with ξ cancels, that is when ξ is parallel to the vector

$$\boldsymbol{n} = \left(\left(\omega_1/k_1^2\right)\boldsymbol{k}_1\cdot\boldsymbol{k}_2 - \omega_2\right)\boldsymbol{k}_1 + \left(\left(\omega_2/k_2^2\right)\boldsymbol{k}_1\cdot\boldsymbol{k}_2 - \omega_1\right)\boldsymbol{k}_2,$$

except when $\boldsymbol{k}_2 = -\boldsymbol{k}_1$ (standing wave) for which $\boldsymbol{n} \perp \boldsymbol{k}_1$ and $\boldsymbol{k}_2$.

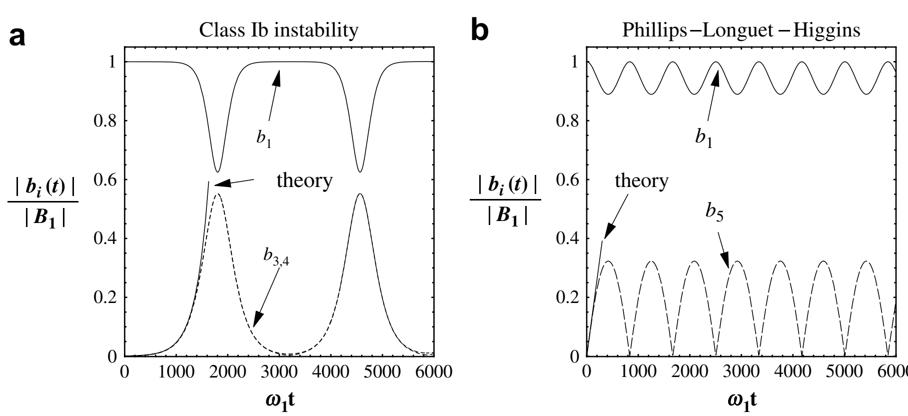

Fig. 8. Nonlinear evolution of bichromatic waves $\boldsymbol{k}_1 = (k_1, 0)$ and $\boldsymbol{k}_2/k_1 = (0, 0.332)$ with initial steepnesses $k_1a_1 = k_2a_2 = 0.1$ interacting with: a class Ib modulation defined by $2\boldsymbol{k}_1 = \boldsymbol{k}_3 + \boldsymbol{k}_4$ with $\boldsymbol{k}_3/k_1 = (1.17, 0)$, (a); a tertiary wave defined by $\boldsymbol{k}_5 = 2\boldsymbol{k}_1 - \boldsymbol{k}_2$, (b).

A sufficient condition of instability for the bichromatic wave train (3) is then:

$$4|T_{12}||B_1||B_2| > k_1^3|B_1|^2 + k_2^3|B_2|^2. \tag{18}$$

Unstable regions according to (18) are represented in Fig. 4: they are islands surrounding the loci of Stokes and standing waves. It can be shown that when $\boldsymbol{k}_1=\boldsymbol{k}_2$ and $a_1=a_2$ (short-crested waves), long wavelength modulations are unstable for $0^\circ \le \theta \le 53.46^\circ$ or $136.06^\circ \le \theta \le 180^\circ$ in agreement with Roskes [15], θ being the angle between $\boldsymbol{k}_1$ and $\boldsymbol{k}_2$. If the primary waves have different steepnesses, long modulations disappear when $(k_2a_2)/(k_1a_1) \le 0.25$.

Class Ia instabilities are plotted in Fig. 5 for different orientations of primary waves with same wavelength and steepness. (We remind that for $\theta=0^\circ$, the corresponding result for Stokes wave with steepness $k_0a_0=k_1a_1+k_2a_2=0.2$ is plotted in Fig. 1a.) As expected, instability remains in the vicinity of the resonant curves (16). As plotted in Fig. 3 already mentioned, the growth rate is minimum for nearly perpendicular waves and maximum for nearly parallel or antiparallel waves. These features are consistent with previous results [22,23].

Turning to cases were wavelengths are different, it can be seen in Fig. 6 that for any orientation, the growth rate decreases with the ratio k_2/k_1. This contrasts with the behavior of class Ib instability which is affected nor by the wavelength ratio nor by orientation. Therefore, approximately when $k_2/k_1 \le 0.3$, class Ia is dominated by class Ib for any orientation of $(\boldsymbol{k}_1,\boldsymbol{k}_2)$.

Long-time evolution of classes Ib and Ia instabilities has been computed numerically from the nonlinear systems (8) and (14) initialized with the most unstable disturbances according to linear theory. As illustrated respectively in Figs. 8a and 10a, the evolutions show the usual recurrences. It is indeed known that system (14) is integrable [9], that and the solution may be expressed in terms of Jacobi elliptic functions [39,40]. This explains recurrence.

6. The resonant interaction of Phillips and Longuet-Higgins

A few years before the discovery of the modulational instability, Phillips [27] and Longuet-Higgins [28] found an explicit configuration in which a nonlinear resonant interaction takes place in a system of three waves, say for convenience $(\boldsymbol{k}_1,\boldsymbol{k}_2,\boldsymbol{k}_5)$. This interaction is best explained as follows [3]: consider a bichromatic wave train $(\boldsymbol{k}_1,\boldsymbol{k}_2)$ as given by (3), and suppose that a disturbance k_5 interacts nonlinearly such that $2\boldsymbol{k}_1 = \boldsymbol{k}_2+\boldsymbol{k}_5$. The Zakharov equation then yields:

$$\left.\begin{aligned} i\dot{b}_1 &= \Gamma_1 b_1 + 2T_{1125}b_1^* b_2 b_5,\\ i\dot{b}_2 &= \Gamma_2 b_2 + T_{1125}b_5^* b_1^2,\\ i\dot{b}_5 &= \Gamma_5 b_5 + T_{1125}b_2^* b_1^2, \end{aligned}\right\} \tag{19}$$

If initially $|b_5| \ll \inf\{|b_1|,|b_2|\}$ and if we set

$$b_5(t) = B_5(t)\mathrm{e}^{-i\Omega_5 t}, \quad \Omega_5 = \omega_5 + 2T_{51}|B_1|^2 + 2T_{52}|B_2|^2$$

the linear evolution of the disturbance is described by

$$i\dot{B}_5 = T_{1125}B_2^* B_1^2 \mathrm{e}^{-i\Delta_{1125}t},$$

and its amplitude is bounded except when $\Delta_{1125}=0$: in that case, growth is linear (not exponential) and happens in the vicinity of the curves

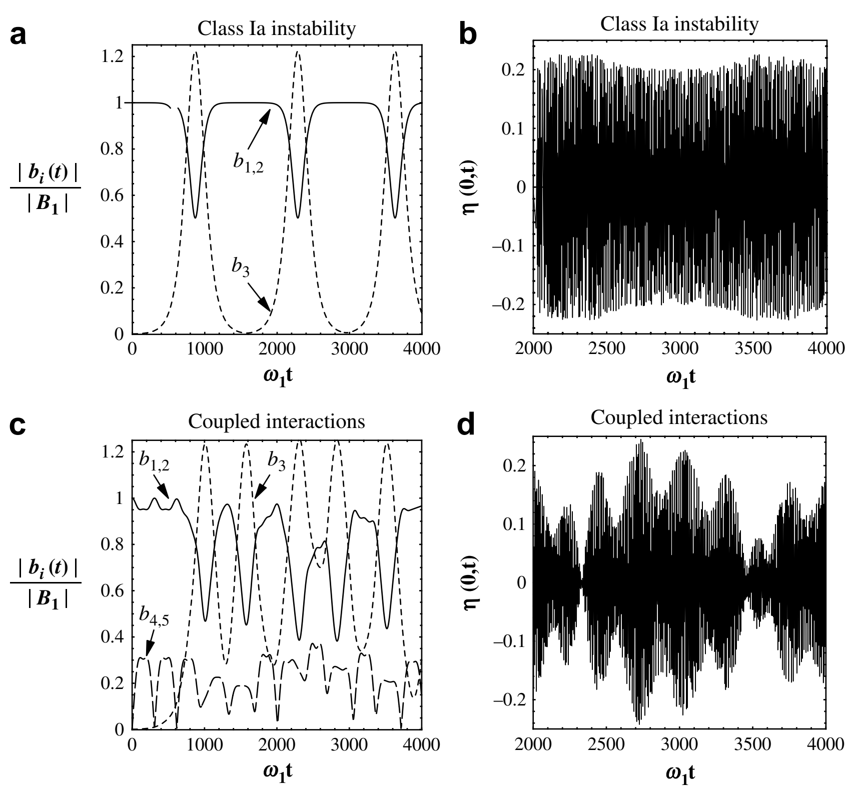

Fig. 10. Nonlinear evolution of bichromatic waves with $k_1=k_2$, $\theta=10^\circ$, $k_1a_1=k_2a_2=0.1$, interacting with: a class Ia modulation defined by $\boldsymbol{k}_3 = \frac{1}{2}(\boldsymbol{k}_1+\boldsymbol{k}_2)$, (a) and (b); three waves $(\boldsymbol{k}_3,\boldsymbol{k}_4,\boldsymbol{k}_5)$ satisfying (21), (c) and (d).

$$2\boldsymbol{k}_1 = \boldsymbol{k}_2 + \boldsymbol{k}_5, \quad 2\omega_1 = \omega_2 + \omega_5, \tag{20}$$

represented in Fig. 7. In terms of amplitude of surface elevation, this gives:

$$a_5(t)/a_1 = \frac{1}{2}(k_1a_1)(k_2a_2)(\omega_1 t)F,$$
$$F = \left(T_{1125}/k_1^3\right)(k_5/k_1)^{1/4}(k_2/k_1)^{-5/4},$$

where a_1 and a_2 are the amplitudes of the undisturbed primary waves.

This mechanism of linear growth with time of the third wave $\boldsymbol{k}_5$ was predicted by Phillips [27] but the coupling coefficient F has been evaluated by Longuet-Higgins [28]. For instance, when the primary waves are perpendicular, the nontrivial solution of (20) is $k_2/k_1 = 0.332$ so that $T_{1123}/k_1^3 = 1.794$ and $F = 0.311$. Longuet-Higgins [28] then proposed an experimental set-up to check the validity of the theory. Experiments have been carried out independently by Longuet-Higgins and Smith [30] and by McGoldrick et al. [31]. Results, summarized by Phillips [3], are in excellent agreement with theory.[1]

These experiments proving for the first time the existence of nonlinear resonant interactions in deep-water gravity waves raise however an important question: why did they not reveal the development of modulational instabilities? The configuration of the primary waves ($\theta = 90^\circ$) is not favorable to class Ia but class Ib is still active. Indeed, with $k_2/k_1 = 0.332$ and $k_1a_1 = k_2a_2 = 0.1$ that correspond to the experimental conditions of McGoldrick et al. [31], the dimensionless growth rates σ_{max}/ω_1 are respectively 0.96×10^{-3} and 4.04×10^{-3} for class Ia and Ib. Thus modulational instability is expected for $\boldsymbol{k}_1$.

To understand, numerical integrations of the nonlinear systems (8) and (19) have been performed to compare the long-time evolution of modulational instability and of the Phillips–Longuet-Higgins resonant interaction. The initial steepness of the disturbance have been chosen as $k_3a_3 = k_4a_4 = 10^{-4}$, a level that may be deduced from the experimental data [31]. Results plotted in Fig. 8 show surprisingly that in the range where linear growth operates for the resonance (20), $\omega_1 t \leq 100$ approximately, the modulational instability remains at a very low level. Since the experimental measures were precisely in this range (converted in fetch), this explains why no modulation has been observed. In other words, tanks were not long enough. Another interesting feature in Fig. 8b is the periodicity of $\boldsymbol{k}_5$ but, contrary to class Ia or Ib modulations, the period is independent of the initial level of the disturbance.

7. Coupling between interactions

Another question then raises: does the induced resonant wave $\boldsymbol{k}_5$ alters modulational instability? To answer this question, interactions have been coupled and the resulting equations solved numerically.

Longuet-Higgins [28] showed that the highest amplifications for the induced resonant wave $\boldsymbol{k}_5$ are reached for small angles between $\boldsymbol{k}_1$ and $\boldsymbol{k}_2$ (the maximum is at $\theta = 17^\circ$). For such angles the primary waves are nearly parallel and have nearly the same wavelength. Therefore it is expected that the resonant mechanism operates not only along the resonant curve but also off-resonance in a small region surrounding the intersection of the two loops of the figure-of-eight.

As an illustration, long-crested waves with $\theta = 10^\circ$ are considered now. As expected, the interaction $2\boldsymbol{k}_1 = \boldsymbol{k}_2 + \boldsymbol{k}_5$ is effective (not shown) even though the initial evolution of the induced wave $\boldsymbol{k}_5$ is not linear as in the exactly resonant case. By symmetry, since $\boldsymbol{k}_2 \simeq \boldsymbol{k}_1$, another induced wave, say $\boldsymbol{k}_4$, grows by the same mechanism if $2\boldsymbol{k}_2 = \boldsymbol{k}_1 + \boldsymbol{k}_4$. Furthermore, Fig. 3 shows that a class Ia modulation should also develop. From (15), the most unstable disturbance is such that $\boldsymbol{k}_3 = \frac{1}{2}(\boldsymbol{k}_1 + \boldsymbol{k}_2)$. But it is now clear that the new implicit interaction $\boldsymbol{k}_1 + \boldsymbol{k}_2 = \boldsymbol{k}_4 + \boldsymbol{k}_5$ has to be taken into account (Fig. 9). To summarize, the quintet of waves $(\boldsymbol{k}_1, \ldots, \boldsymbol{k}_5)$ satisfying:

$$\boldsymbol{k}_1 + \boldsymbol{k}_2 = 2\boldsymbol{k}_3, \quad 2\boldsymbol{k}_2 = \boldsymbol{k}_1 + \boldsymbol{k}_4, \quad 2\boldsymbol{k}_1 = \boldsymbol{k}_2 + \boldsymbol{k}_5,$$
$$\boldsymbol{k}_1 + \boldsymbol{k}_2 = \boldsymbol{k}_4 + \boldsymbol{k}_5, \tag{21}$$

is governed by the system:

$$i\dot{b}_1 = \Gamma_1 b_1 + 2T_{1245} b_2^* b_4 b_5 + 2T_{1125} b_1^* b_2 b_5 + T_{2214} b_4^* b_2^2 + T_{1233} b_2^* b_3^2,$$
$$i\dot{b}_2 = \Gamma_2 b_2 + 2T_{1245} b_1^* b_4 b_5 + 2T_{2214} b_2^* b_1 b_4 + T_{1125} b_5^* b_1^2 + T_{1233} b_1^* b_3^2,$$
$$i\dot{b}_3 = \Gamma_3 b_3 + 2T_{1233} b_3^* b_1 b_2,$$
$$i\dot{b}_4 = \Gamma_4 b_4 + 2T_{1245} b_5^* b_1 b_2 + T_{2214} b_1^* b_2^2,$$
$$i\dot{b}_5 = \Gamma_5 b_5 + 2T_{1245} b_4^* b_1 b_2 + T_{1125} b_2^* b_1^2.$$

Numerical results are plotted in Fig. 10c and d showing the destruction of recurrence and the great variability of the free-surface elevation.

8. Discussion

Classes Ia and Ib modulations in bichromatic wave trains have been characterized with the Zakharov equation. Explicit expressions for growth rates have been derived; these are valid for any amplitudes, wavelengths, and directions of propagation.

The effect of the resonant interaction of Phillips and Longuet-Higgins on the evolution of these modulations has been discussed. When activated, this resonance destroys the recurrent evolution of quartets. This is in particular the case when two primary waves with close or equal wavelengths cross each other at a small angle (long-crested waves).

However, laboratory experiments by Hammack, Henderson and Segur [41] on bichromatic waves similar to those studied here show none of the features presented in Fig. 10. Rather, the waves are stable and persistent thanks to dissipation [19]. Numerical inviscid simulations by Fuhrman et al. [42] show the development and the (quasi) recurrent evolution of class Ia and Ib modulations in long-crested waves, but again no resonant interaction of the kind discussed in Sections 6 and 7 seems observed. This is perhaps due to the initialization of the computations [43].

Acknowledgments

This work has been supported by INSU. I am grateful to the referees for their constructive criticisms. This paper is dedicated to Georges Perec.

Appendix : Krasitskii's kernel

Here is Krasitskii's kernel $T(\boldsymbol{k}_a, \boldsymbol{k}_b, \boldsymbol{k}_c, \boldsymbol{k}_d) = T_{abcd}$ as given in Ref. [12]. Note that Janssen's convention for the Fourier transform is used here so that Krasitskii's original expressions are divided here by $(2\pi)^2$.

[1] It is worthy to note that the mechanism of Phillips and Longuet-Higgins is not an instability in the usual mathematical sense since $b_5(t) = 0$ and $b_1(t)$, $b_2(t)$ given by (3) is *not* a solution to (19), while for instance $b_3(t) = b_4(t) = 0$ and $b_1(t)$, $b_2(t)$ given by (3) *is* a solution to system (14). Rather, it is the response of the three-wave system (19) to prescribed initial data with $b_5(0) = 0$. I am grateful to a referee for pointing to me out this subtelty.

$$T_{abcd} = U_{-a,-b,c,d} + U_{c,d,-a,-b} - U_{c,-b,-a,d} - U_{-a,c,-b,d} - U_{-a,d,c,-b} - U_{d,-b,c,-a}$$
$$-V^{-}_{a,c,a-c}V^{-}_{d,b,d-b}\left\{(\omega_c+\omega_{a-c}-\omega_a)^{-1}+(\omega_b+\omega_{d-b}-\omega_d)^{-1}\right\}$$
$$-V^{-}_{b,c,b-c}V^{-}_{d,a,d-a}\left\{(\omega_c+\omega_{b-c}-\omega_b)^{-1}+(\omega_a+\omega_{d-a}-\omega_d)^{-1}\right\}$$
$$-V^{-}_{a,d,a-d}V^{-}_{c,b,c-b}\left\{(\omega_d+\omega_{a-d}-\omega_a)^{-1}+(\omega_b+\omega_{c-b}-\omega_c)^{-1}\right\}$$
$$-V^{-}_{b,d,b-d}V^{-}_{c,a,c-a}\left\{(\omega_d+\omega_{b-d}-\omega_b)^{-1}+(\omega_a+\omega_{c-a}-\omega_c)^{-1}\right\}$$
$$-V^{-}_{+a+b,a,b}V^{-}_{+c+d,c,d}\left\{(\omega_{a+b}-\omega_a-\omega_b)^{-1}+(\omega_{c+d}-\omega_c-\omega_d)^{-1}\right\}$$
$$-V^{+}_{-a-b,a,b}V^{+}_{-c-d,c,d}\left\{(\omega_{a+b}+\omega_a+\omega_b)^{-1}+(\omega_{c+d}+\omega_c+\omega_d)^{-1}\right\},$$
$$U_{a,b,c,d} = \frac{1}{16}\left(\frac{\omega_a\omega_b}{\omega_c\omega_d}k_ak_bk_ck_d\right)^{\frac{1}{2}}(2k_a+2k_b-k_{b+d}-k_{b+c}-k_{a+d}-k_{a+c}),$$
$$V^{\pm}_{a,b,c} = \frac{\sqrt{2}}{8}\left\{\left(\frac{\omega_a\omega_bk_c}{\omega_ak_bk_c}\right)^{\frac{1}{2}}W^{\pm}_{a,b}+\left(\frac{\omega_a\omega_ck_b}{\omega_bk_ak_c}\right)^{\frac{1}{2}}W^{\pm}_{a,c}+\left(\frac{\omega_b\omega_ck_a}{\omega_ak_bk_c}\right)^{\frac{1}{2}}W^{+}_{b,c}\right\},$$
$$W^{\pm}_{a,b} = \boldsymbol{k}_a\cdot\boldsymbol{k}_b \pm k_ak_b, \quad \omega_{a\pm b} = \omega(\boldsymbol{k}_a\pm\boldsymbol{k}_b), \quad k_{a\pm b} = |\boldsymbol{k}_a\pm\boldsymbol{k}_b|.$$

Recall that the transfer function obeys the symmetries: $T_{abcd}=T_{bacd}=T_{abdc}=T_{cdab}$ [32], and that in deep water: $T_{aaaa}=k_a^3$ and T_{abab} is given by (4).

References

[1] T.B. Benjamin, F.E. Feir, The disintegration of wave trains on deep water. Part 1, J. Fluid Mech. 27 (1967) 417–430.
[2] D.J. Benney, A.C. Newell, The propagation of nonlinear wave envelopes, J. Math. Phys. 46 (1967) 133–145.
[3] O.M. Phillips, Theoretical and experimental studies of gravity wave interactions, Proc. R. Soc. Lond. A 299 (1967) 104–119.
[4] V.E. Zakharov, Stability of periodic waves of finite amplitude on the surface of deep fluid, J. Appl. Mech. Tech. Phys. 2 (1968) 190–194.
[5] D.R. Crawford, B.M. Lake, P.G. Saffman, H.C. Yuen, Stability of weakly nonlinear deep-water waves in two and three dimensions, J. Fluid Mech. 14 (1981) 577–584.
[6] M.S. Longuet-Higgins, The instabilities of gravity waves of finite amplitude in deep water. Part 1, Proc. R. Soc. Lond. A 360 (1978) 471–488.
[7] O.M. Phillips, Wave interactions—the evolution of an idea, J. Fluid Mech. 106 (1981) 215–227.
[8] H.C. Yuen, B.M. Lake, Nonlinear dynamics of deep-water gravity waves, Adv. Appl. Mech. 22 (1982) 67–229.
[9] A.D.D. Craik, Wave interactions and fluid flows, Cambridge University Press, 1985.
[10] L. Shemer, M. Stiassnie, The Zakharov and modified Zakharov equations and their applications, in: A.R. Osborne (Ed.), Nonlinear topics in ocean physics, Italian Physical Society, 1988, pp. 581–620.
[11] F. Dias, C. Kharif, Nonlinear gravity and capillary-gravity waves, Annu. Rev. Fluid Mech. 31 (1999) 301–346.
[12] P. Janssen, The Interaction of ocean waves and wind, Cambridge University Press, 2004.
[13] V.E. Zakharov, L.A. Ostrovsky, Modulation instability: the beginning, Physica D 238 (2009) 540–548.
[14] T.J. Bridges, A. Mielke, A proof of the Benjamin–Feir instability, Arch. Rat. Mech. Anal. 133 (1995) 145–198.
[15] G.J. Roskes, Nonlinear multiphase deep-water wavetrains, Phys. Fluids 19 (1976) 1253–1254.
[16] A.K. Dhar, K.P. Das, Fourh-order nonlinear evolution equation for two Stokes wave trains in deep water, Phys. Fluids A 3 (1991) 3021–3026.
[17] R.D. Pierce, E. Knobloch, On the modulational stability of traveling an standing water waves, Phys. Fluids 6 (1994) 1177–1190.
[18] M. Onorato, A.R. Osborne, M. Serio, Modulational instability in crossing sea states: a possible mechanism for the formation of freak waves, Phys. Rev. Lett. 96 (2006) 014503 (4 pages).
[19] W. Craig, D.M. Henderson, M. Oscamou, H. Segur, Stable three-dimensional waves of nearly permanent form on deep water, Math. Comput. Simul. 74 (2007) 135–144.
[20] M. Okamura, Instabilities of weakly nonlinear standing gravity waves, J. Phys. Soc. Jap. 53 (1984) 3788–3796.
[21] M. Ioualalen, C. Kharif, Stability of three-dimensional progressive gravity waves on deep water to superharmonic disturbances, Eur. J. Mech. B/Fluids 12 (1993) 401–414.
[22] M. Ioualalen, C. Kharif, On the subharmonic instabilities of steady three-dimensional deep water waves, J. Fluid Mech. 262 (1994) 265–291.
[23] S.I. Badulin, V.I. Shrira, C. Kharif, M. Ioualalen, On two approaches to the problem of instability of short-crested water waves, J. Fluid Mech. 303 (1995) 297–326.
[24] O. Kimmoun, M. Ioualalen, C. Kharif, Instabilities of steep short-crested surface waves in deep water, Phys. Fluids 11 (1999) 1679–1681.
[25] T.J. Bridges, F.E. Laine-Pearson, Nonlinear counter propagating waves, multi-sympletic geometry, and the instability of standing waves, SIAM J. Appl. Math. 64 (2004) 2096–2120.
[26] T.J. Bridges, F.E. Laine-Pearson, The long-wave instability of short-crested waves, via embedding in a oblique two-wave interaction, J. Fluid Mech. 543 (2005) 147–182.
[27] O.M. Phillips, On the dynamics of unsteady gravity waves of finite amplitude. Part 1, J. Fluid Mech. 9 (1960) 193–217.
[28] M.S. Longuet-Higgins, Resonant interactions between two trains of gravity waves, J. Fluid Mech. 12 (1962) 321–332.
[29] M.S. Longuet-Higgins, O.M. Phillips, Phase velocity effects in tertiary wave interactions, J. Fluid Mech. 12 (1962) 333–336.
[30] M.S. Longuet-Higgins, N.D. Smith, An experiment on third-order resonant wave interactions, J. Fluid Mech. 25 (1966) 417–435.
[31] L.F. McGoldrick, O.M. Phillips, N.E. Huang, T.H. Hodgson, Measurements of third-order resonant wave interactions, J. Fluid Mech. 25 (1966) 437–456.
[32] V.P. Krasitskii, On reduced equations in the Hamiltonian theory of weakly nonlinear surface waves, J. Fluid Mech. 272 (1994) 1–20.
[33] S.J. Hogan, I. Gruman, M. Stiassnie, On the changes in phase speed of one train of water waves in the presence of another, J. Fluid Mech. 192 (1988) 97–114.
[34] A.J. Roberts, D.H. Peregrine, Notes on long-crested water waves, J. Fluid Mech. 135 (1983) 323–335.
[35] D.J. Benney, Non-linear gravity wave interactions, J. Fluid Mech. 14 (1962) 577–584.
[36] K. Hasselmann, On the non-linear energy transfer in a gravity-wave spectrum. Part 1, J. Fluid Mech. 12 (1962) 481–500.
[37] K. Hasselmann, On the non-linear energy transfer in a gravity-wave spectrum. Part 2, J. Fluid Mech. 15 (1963) 273–281.
[38] K. Hasselmann, On the non-linear energy transfer in a gravity-wave spectrum. Part 3, J. Fluid Mech. 15 (1963) 385–398.
[39] F.P. Bretherton, Resonant interactions between waves. The case of discrete oscillations, J. Fluid Mech. 20 (1964) 457–480.
[40] M. Stiassnie, L. Shemer, On the interaction of four water waves, Wave Motion 41 (2005) 307–328.
[41] J.L. Hammack, D.M. Henderson, H. Segur, Progressive waves with persistent two-dimensional surface patterns in deep water, J. Fluid Mech. 532 (2005) 1–52.
[42] D.R. Fuhrman, P.A. Madsen, H.B. Bingham, Numerical simulation of lowest-order short-crested wave instabilities, J. Fluid Mech. 563 (2006) 415–441.
[43] D. Harvar, B.C.P. Mercy, Personnal communication, 2009.